RELEASE CHARACTERISTICS OF PROTEIN DRUGS FROM DNA HYDROGELS

A Thesis

Presented to the Faculty of the Graduate School

of Cornell University

In Partial Fulfillment of the Requirements for the Degree of

Master of Science

by

Ying Liu

August 2007

ABSTRACT

DNA molecules have been used as generic instead of genetic materials to construct nanostructures. Based on Watson-Crick base pairing, a three-arm junction DNA, or Y-shaped DNA (Y-DNA), was first synthesized from three partially complementary oligonucleotides as a basic building block. Each Y-DNA consists of three non-palindromic sticky ends so that it could ligate to other DNA building blocks to form desired nanostructures and DNA hydrogel.

The goal of this work was to utilize DNA hydrogel as a protein drug delivery system. In previous work, we created DNA hydrogels that had good swelling abilities, controlled degradation rates and were cytocompatible. In the present studies, we characterized the release of two model proteins, insulin and bovine serum albumin (BSA), from DNA hydrogels. A numerical simulation of the whole release system based on a FEM method was achieved. These initial studies indicate that DNA hydrogels are suitable for delivering proteins for controlled drug delivery and tissue engineering.

BIOGRAPHICAL SKETCH

Born and raised in Wuhan, a city in central China with a population of eight million, Ying Liu was very enthusiastic to all living things. He chose Electronic Information Engineering as his major after he graduated from Wuhan Foreign Language School. After a four-year fruitful college study in Wuhan Univerisity, Ying obtained his Bachelor of Engineering degree in Electronic Information Engineering with honor. Then he went to Singapore for his graduate study in the Graduate Program in Bioengineering at the National University of Singapore. He successfully completed all the coursework and research project.

In July 2005, Ying went to Cornell University in the USA for his graduate study. He studied under the direction of Professor Dan Luo in the Department of Biological and Environmental Engineering. After a two-year hard work, Ying is trying to seek a position in pharmaceutical industry utilizing his background in both biology and engineering.

ACKNOWLEDGMENTS

Many people have provided me tremendous help along the journey to complete my study at Cornell. Without their friendship, encouragement and guidance, 2007 would not have seen this dissertation.

First, I would like to offer my sincere thanks to Professor Dan Luo, my academic advisor and the chair of my committee. I feel so lucky to work with such a professor who selflessly devotes his professional talent, time and energy to his students. I have been benefiting from his advice, in both profession and life. His detail-oriented work attitude and perfectionism will have a great influence on my future. I am also indebted to the other members in my committee, Professor Ashim Datta, for willing to serve as my committee members and for his constructive suggestions during my study at Cornell. Both of my advisors have provided me with every opportunity a graduate student could hope for and I thank them both for this.

I also acknowledge the help of Dr. E. Balsa-Canto and Dr. J. Banga of the Process Eng. Group, I.I.M.- C.S.I.C, Vigo, Spain, for their supporting work in the area of optimization. Their work nicely complemented my model.

My research project could not have been possible without the support of the entire Molecular Bioengineering Lab. I would like to especially thank Soong Ho Um for his amazing research mentorship and for his friendship. In addition to those who directly participated in my research project, I would like to thank my Biological and Environmental Engineering support staff: Professor John March and Brenda Marchewka.

This research would not have been possible without the assistance and support from the other members in the Molecular Bioengineering Lab, Hisa, Nokyoung, Wenlong, Jay, Liang, JB, Sang, Thua, Hoon, Mike, and Natt. You guys are great; you made the

time here at Cornell much more enjoyable. I thank you and wish you the best in your careers.

As always, I owe heartfelt thanks to my family for their love, encouragement and support. I give my appreciation to my parents, Jingsheng Liu and Wenjuan Yu, for their unconditional love and support.

Finally I would like to thank that special person in my life. Junping has been by my side for much of graduate work. It is her motivation that has kept me on track. She is the driving force in my life, always helping me to achieve my goals.

TABLE OF CONTENTS

LIST OF FIGURES

LIST OF TABLES

LIST OF ABBREVIATIONS

DL-DNA - Dendrimer-like DNA

BSA - Bovine Serum Albumin

BDM - Branched DNA monomer

PBS- Phosphate Buffer Saline

ELSIA- Enzyme-linked ImmunoSorbent Assay

ss-DNA- Single-stranded DNA

PLG- Poly (lactide-glycolides)

Mw-Molecular Weight

FEM- Finite Element Method

CHAPTER 1
Introduction: Branched DNA Molecules and DNA Hydrogel

1.1 Branched DNA molecules

DNA molecules are well known as genetic information carriers and the core of the central dogma. A naturally existing DNA molecule is an either linear or circular polymer with a backbone of alternating phosphate and carbon sugar (deoxyribose), which is attached to a base, adenine (A), guanine (G), cytosine (C), or thymine (T). A single-stranded DNA (ssDNA) is chemically polar with a 5' phosphorylated end (the phosphate group on the 5' carbon of the sugar ring) and 3' hydroxyl end (the hydroxyl group on the 3' carbon of the sugar ring). The presence of chemically active 5' phosphate and 3' hydroxyl functional groups offer great possibility to functionalize DNA with many chemical entities, including proteins, fluorochromes, and metals. Use of nucleic acids as generic materials instead of genetic materials has sparked much research interest in recent years. Many DNA nanotechnology advances have been made by Seeman and colleagues, including the creation of various geometric objects, periodic frameworks, arrays, and scaffolds using 'double crossover' DNA[1]. Other progress has also been made with linear DNA in developing systems such as biotin-avidin based gene networks, DNA conjugated Au nanocrystals, DNA-templated Au wires, and hybrid DNA-protein nanocomplexes[1, 4, 5]. However, all these advances have utilized linear DNA, restricting their effectiveness in molecular constructions[1]. To overcome this limitation, DNA building blocks of different shapes must be constructed with the ability to be incorporated into larger schemes in a controlled manner[1].

In 2004, Luo and colleagues created a new DNA building block in the shape of the letter Y[2]. These Y-DNA building blocks are designed to have specific sticky ends, allowing them to specifically and covalently attach to other Y-DNAs in a controlled and enzyme-catalyzed means[2]. When the Y-DNAs are specifically attached to each other, they form a multivalent and anisotropic dendrimer-like structure, named

dendrimer-like DNA (DL-DNA; Figure 1.1)[2].

There are many possible applications for DL-DNA, including a potential drug carrier, a multi-gene therapy vector, and a DNA nanobarcode[1, 2, 3].

In a similar manner, X-DNAs and T-DNAs can be synthesized from X-DNA building blocks and T-DNA building blocks, respectively. In 2006, Luo and colleagues created DNA hydrogels from branched DNA monomers (BDM)[3]. DNA hydrogels were created using anisotropic DNA building blocks as shown in Figure 1.2. Different DNA hydrogels are possible to create because DNA building blocks can be different. Also the geometry and dimensions of DNA hydrogels can be exactly controlled (Figure 1.3)[2].

In this project, the potential of using DNA hydrogel as a drug carrier was explored, specifically for two protein drugs, insulin and bovine serum albumin (BSA).

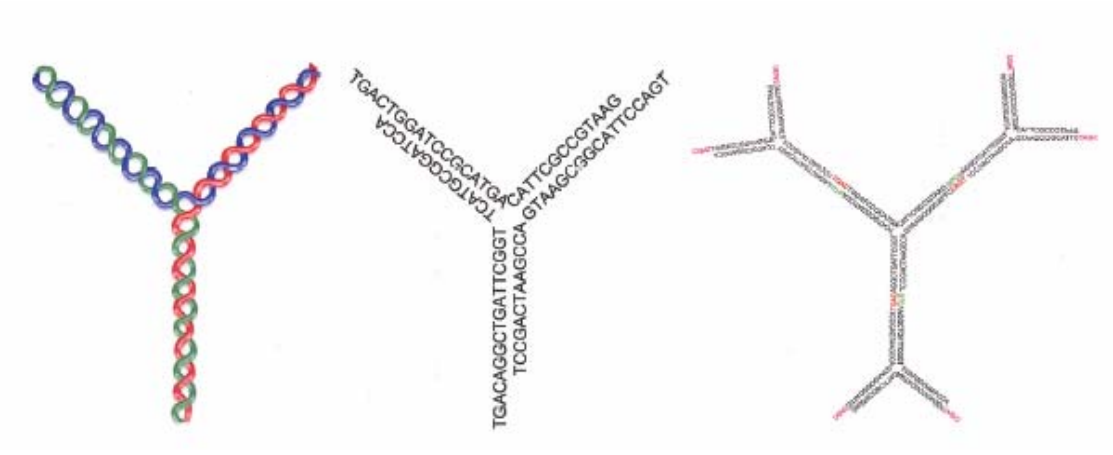

Figure 1.1. – (left) Schematic drawing of Y-shaped DNA. (middle) Actual single strand DNA sequences. (right) DL-DNA formed by four Y-shaped DNA building blocks[1].

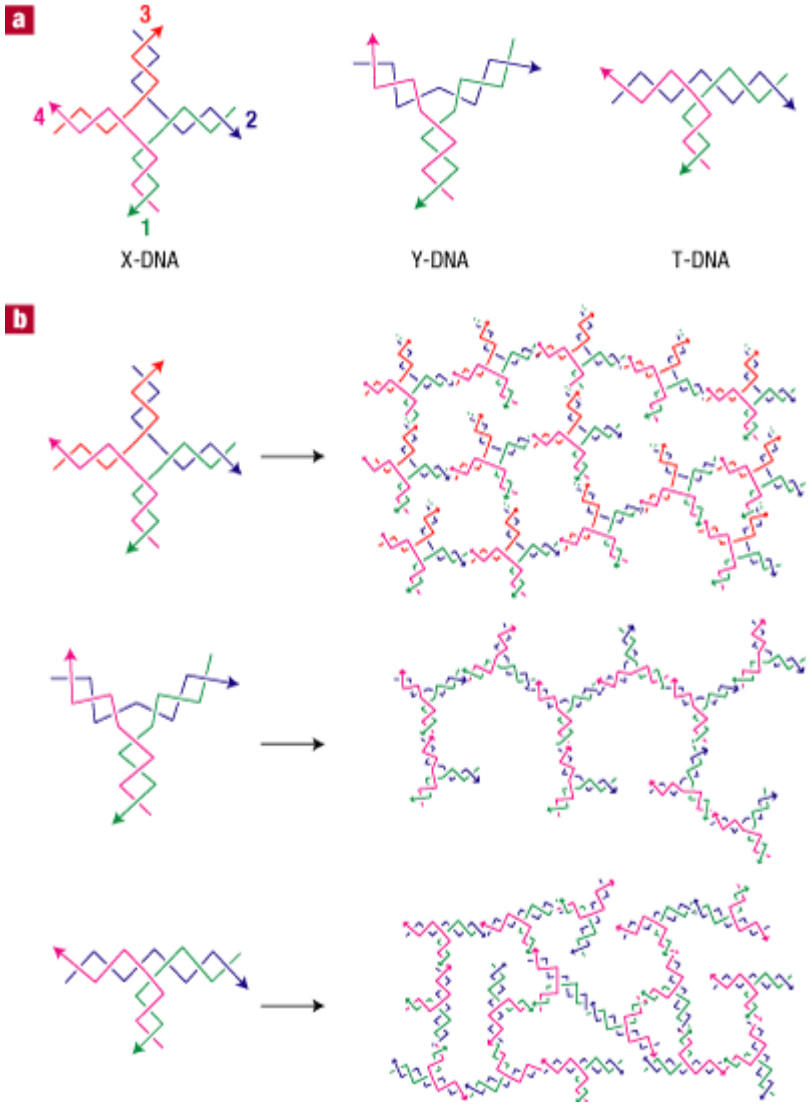

Figure 1.2. Schematic Diagram of synthesis of different DNA hydrogels from X-DNA, Y-DNA, and T-DNA building blocks, respectively[2].

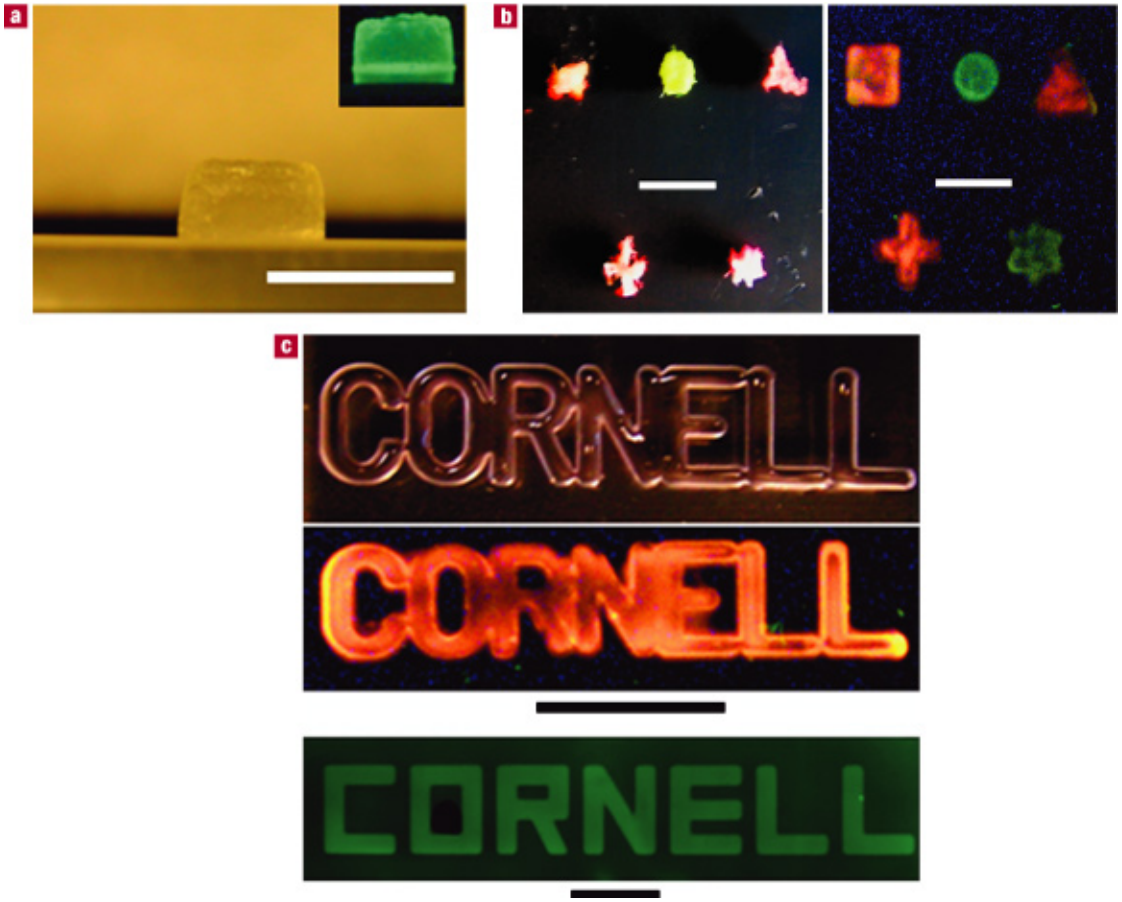

Figure 1.3. Hydrogels made entirely from branched DNA. **a**, A swollen X-DNA hydrogel fabricated in a cylindrical mould. The size is 7.0 mm in diameter and 3.0 mm in height. The scale bar is 1 cm. The inset shows the DNA gel stained with SYBR I. **b**, Images of dried (left) and swollen (right) X-DNA hydrogels with different patterns: rectangular, circular, triangular, star and cross (from the top left corner, clockwise). The scale bars are 1 cm. **c**, X-DNA gels patterned in CORNELL shapes at centimetre scale (top and middle rows; the scale bar is 1 cm) and micrometre scale (bottom row; the scale bar is 500 μm). They were stained with two different, DNA-specific fluorescent dyes: ethidium bromide (red, the middle row) and SYBR I (green, the bottom row).

1.2 DNA hydrogel

A hydrogel is a three-dimensional polymer network of hydrophilic polymer chains that are crosslinked through either chemical or physical bonding. Because of the hydrophilic nature of polymer chains, hydrogels absorb water to swell in the presence of abundant water. The swelling process is the same as the dissolution of non-crosslinked hydrophilic polymers. By definition, water constitutes at least 10% of the total weight (or volume) of a hydrogel. When the content of water exceeds 95% of the total weight (or volume), the hydrogel is called a superabsorbent. Because measuring the weight of a swelling hydrogel is much easier than measuring the volume, the swelling ratio of hydrogels is usually expressed based on weights. In a chemical hydrogel, all polymer chains are crosslinked to each other by covalent bonds, and thus, the hydrogel is one molecule regardless of its size. For this reason, there is no concept of molecular weight of hydrogels, and hydrogels are sometimes called infinitely large molecules or supermacromolecules. One of the unique properties of hydrogels is their ability to maintain original shape during and after swelling due to isotropic swelling.

Hydrogels have been used widely in the development of biocompatible biomaterials, and this is mainly due to the low interfacial tension and low frictional surface by the presence of water on the surface. The dried hydrogels (also called xerogels) are usually clear, and swelling in water takes a long time. The slow swelling process is due to slow diffusion of water through the compact polymer chains. It is this slow swelling property that has been useful in controlled drug delivery. For a glassy hydrogel of a size equivalent to a stack of five pennies, it will take hours before the hydrogel shows appreciable swelling.

Hydrogels are very versatile materials and have attracted significant attention recently as drug delivery systems. In addition to their inertness and good compatibility, the

ability of hydrogels to release an entrapped drug in an aqueous medium and the ease of regulating such drug release make hydrogels particularly suitable as drug carriers for the controlled release of pharmaceuticals. First, there is no need to remove residual biomaterials from the implant site to improve tissue compatibility. Secondly, biodegradable hydrogels allow a wider range of drug release profiles and hence more versatile. Therefore, a biodegradable hydrogel delivery system appears to be one of the most promising approaches for protein delivery. Biodegradable hydrogels would permit then entrapped proteins to be released in a controlled manner through both drug diffusion and hydrogel degradation. Such a combination of diffusion and degradation controlled mechanisms may provide us with the desirable release kinetics of proteins that have a wide range of molecular sizes.

Several strategies and materials have been employed as hydrogel drug delivery systems for protein drugs. For instance, synthetic biodegradable polymers, such as poly (lactide-glycolides) (PLG) or polyanhydrides can be used for controlled release of pharmaceutical substances including bioactive macromolecules. Due to the use of organic solvents, incorporation of biologically active molecules into these hydrogel systems often results in their inactivation. Recently, DNA hydrogels have been made[3]. These DNA hydrogels have been synthesized in a mild condition and they have been shown to be biodegradable, biocompatible and non-toxic to mammalian cells. In addition, DNA hydrogels have great swelling abilities and moderate mechanical properties. These make DNA hydrogels as very interesting controlled release systems.

The purpose of the present study was to evaluate the in vitro release kinetics of protein drugs from different DNA hydrogels in order to understand the mechanism of release and explore the potential application of DNA hydrogels as drug delivery systems. In this study, we chose insulin and bovine serum albumin (BSA) as the model proteins. Due to its importance for therapeutic use in a large and expanding market, insulin has

been the focus of intensive research in both academia and industry. Especially The challenge of administering insulin orally has been addressed over the last several decades with a view to helping ease the pain and stress caused during insulin injections by the millions of diabetic patients worldwide[6]. BSA is a well-studied protein that has been used as a model for controlled release of proteins from hydrogel systems. It is inexpensive, easy to assay and generally available.

REFERENCES

1. D. Luo. The road from biology to materials. *Materials Today*, **6**, 38-43 (2003)
2. Y. Li, Y.D. Tseng, S.Y. Kown, L. d'Espaux, J.S. Bunch, P.L McEuen and D. Luo. Controlled assembly of dendrimer-like DNA. *Nature Materials*, **3**, 38-42 (2004)
3. S. H. Um, J. B. Lee, N. Park, S. Y. Kwon, C. C. Umbach and D. Luo. Enzyme-catalysed assembly of DNA hydrogel, *Nature Materials*, **5**, 797-801 (2006)
4. K. Jain. Nanodiagnostics: application of nanotechnology in molecular diagnostics. *Expert Review of Molecular Diagnostics*, **3** (2), 153-161 (2003)
5. R. Freeman, P. Raju, S. Norton, I. Walton, P. Smith, L. He, M. Nathan, M. Sha, and S. Penn. Use of nanobarcodes particles in bioassays. *Methods in Molecular Biology*, **303**, 73-81 (2005)
6. H. R. Costantino, S. Liauw, S. Mitragotri, R. S. Langer, A. M. Klibanov, and V. Sluzky. The pharmaceutical development of insulin: Historical perspectives and future directions, *Therapeutic protein and peptide formulation and delivery ACS Symposium series*, **675**, 29-66 (1997)

CHAPTER 2
Materials and Methods

2.1 Materials

Porcine insulin (Mw 5770) and bovine serum albumin (BSA, Mw 68,000) were purchased from Sigma Chemicals (St. Louis, MO). DNA oligonucleotides were purchased from IDTDNA (USA). Insulin and BSA solutions were prepared by dissolving the protein powder in milli Q water with designed weight ratio (w/w).

Table 2.1 Sequence of Oligonucleotides

Strand	Segment 1	Segment 2
X_{01}	5'-p-ACGT	CGA CCG ATG AAT AGC GGT CAG ATC CGT ACC TAC TCG-3'
X_{02}	5'-p-ACGT	CGA GTA GGT ACG GAT CTG CGT ATT GCG AAC GAC TCG-3'
X_{03}	5'-p-ACGT	CGA GTC GTT CGC AAT ACG GCT GTA CGT ATG GTC TCG-3'
X_{04}	5'-p-ACGT	CGA GAC CAT ACG TAC AGC ACC GCT ATT CAT CGG TCG-3'
Y_{0a}	5'-p-ACGT	CGA CCG ATG AAT AGC GGT CAG ATC CGT ACC TAC TCG-3’
Y_{0b}	5'-p-ACGT	CGA GTC GTT CGC AAT ACG ACC GCT ATT CAT CGG TCG-3’
Y_{0c}	5'-p-ACGT	CGA GTA GGT ACG GAT CTG CGT ATT GCG AAC GAC TCG-3’
T_{0a}	5'-p-ACGT	CGA CAG CTG ACT AGA GTC ACG ACC TGT ACC TAC TCG-3'
T_{0b}	5'-p-ACGT	CGA GTC GTT CTC AAG ACG TAG CTA GGA CTC TAG TCA GCT GTC G-3'
T_{0c}	5'-p-ACGT	CGA GTA GGT ACA GGT CGT CGT CTT GAG AAC GAC TCG-3’

Table 2.2 Properties of insulin and BSA

	Molecular Weight (Dalton)	Hydrodynamic Radius (nm)	Solubility in Water (mg/ml)
Insulin Monomer	5770	1.3	1
BSA Monomer	68000	3.7	40

2.2 Methods

2.2.1 Preparation of BDM and DNA hydrogel

BDM were designed and synthesized according to the procedures described previously[1].

In brief, X-DNA was constructed by mixing three oligonucleotide components (1:1:1 molar ratio) in sterile Milli-Q water with a final concentration of 5 mM for each oligonucleotide. Hybridizations were performed according to the following procedures: (i)

Denaturation at 95 °C for 2 min. (ii) Cooling at 65 °C and incubation for 5 min. (iii) Annealing at 60 °C for 2 min. (iv) Further annealing at 60 °C for 0.5 min with a continuous temperature decrease at a rate of 1 °C per min. The annealing steps were repeated a total of 40 times. The final annealed products were stored at 4 °C.

DNA hydrogels were synthesized according to the procedures described previously[2]. In brief, to construct an X-DNA gel, branched X-DNA molecules were designed and synthesized, in such a way that each arm of the X-DNA molecule possessed a complementary sticky end whose sequences were palindromic. Thus, these branched X-DNA molecules were able to hybridize to and ligate with each other via T4 DNA

ligase, serving as both monomers and crosslinkers. The self-assembly of branched X-DNA monomers (BDM) coupled with ligase-catalysed reactions led to a large-scale, three-dimensional structure that had the properties of a hydrogel. Each X-DNA molecule was ligated with Weiss unites of T4 DNA ligase (Promega). The reaction was carried out at room temperature overnight on a gentle rotator.

2.2.2 Hydrogel protein release

To characterize the release of model proteins from DNA hydrogels, 0.1% (w/v) insulin and bovine serum albumin (BSA) stock solutions were added in the gelation solution prior to crosslinking. We cross-linked 200 µl of gelation solution in 6-mm diameter, 15-mm deep mold (Company). After overnight gentle shaking, the completely-formed hydrogels were carefully transferred to empty 1.5 ml polypropylene tubes.

After all of the hydrogels were synthesized, they were washed by adding 0.5 ml of phosphate buffered saline (PBS) to the tubes for 3 times. After washing, 0.5 ml of PBS was added to each tube as the release buffer. The tubes were mixed at 50 rpm at 20 °C. At specified sample collection times, 0.5 ml of solution was transferred to a 1.5 ml centrifuge tube and the tube was replenished with 0.5 ml fresh PBS.

For Insulin, the protein content of each sample was analyzed with the Porcine ELISA kit (ALPCO Diagnostics). For BSA, the protein content of each sample was analyzed with the Bio-Rad protein assay using the mircroassay procedure. Triplicate hydrogels were analyzed in each trial.

2.2.3 Computer simulation

To have a mechanistic understanding of the release process, a diffusion model of the protein release through the gel was developed. Figure 3.10 shows a schematic of the system with the boundary conditions. Proteins are assumed to diffuse to the boundary and get convected away by the release buffer. The removal by the release buffer is assumed to be symmetric. The governing equation for diffusion in an axisymmetric cylindrical geometry is

$$\frac{\partial c}{\partial t} = \left[\frac{1}{r} \frac{\partial}{\partial r} \left(rD \frac{\partial c}{\partial r} \right) + \frac{\partial}{\partial z} \left(D \frac{\partial c}{\partial z} \right) \right] \qquad (2.1)$$

Here c is protein concentration; r and z are radial and axial coordinates, respectively. T is time of release. R and H are radius and height of cylinder, respectively, and D is the diffusivity of protein drugs, in the hydrogel, which can be function of concentration.

The release buffer, having zero concentration of proteins, is replaced at two day intervals and is agitated, leading to the boundary condition

$$c(r = R) = 0 \qquad (2.2)$$

Symmetry at the center leads to the following boundary condition at the center

$$\frac{\partial c}{\partial r}(r = 0) = 0 \qquad (2.3)$$

At the top and bottom of the cylinder,

$$c(z = 0) = 0 \qquad (2.4)$$

$$c(z = H) = 0 \qquad (2.5)$$

Initial protein concentration in the hydrogel is $C_{0,}$

$$c(r, z, t = 0) = c_0 \qquad (2.6)$$

The governing equation and boundary conditions were solved in finite element computational software COMSOL (COMSOL, USA). Rectangular elements were

used. The number of elements was increased until it did not affect the solution (called mesh convergence). A total of 625 elements were used for the final computation.

REFERENCES

1. Y. Li, Y.D. Tseng, S.Y. Kown, L. d'Espaux, J.S. Bunch, P.L McEuen and D. Luo. Controlled assembly of dendrimer-like DNA. *Nature Materials*, **3**, 38-42 (2004)

2. S. H. Um, J. B. Lee, N. Park, S. Y. Kwon, C. C. Umbach and D. Luo. Enzyme-catalysed assembly of DNA hydrogel, *Nature Materials*, **5**, 797-801 (2006)

CHAPTER 3
Results and Conclusions

3.1 Results

In the one-pot approach, equal moles of all three oligonucleotides were mixed well together to form Y-DNA. The formation of Y-DNA was evaluated by gel electrophoresis (Figure 3.1), in which the mobility of a DNA molecule depends on its size, shape and extent of base pairing. One major band of each lane appeared on the gel (Figure 3.1A, lane 7), and its mobility was less than that of its components, the single-stranded DNA (Figure 3.1A, lane 6), indicating the formation of one arm of Y-DNA. The further shift of the mobility of the final annealing product of one-pot synthesis (Figure 3.1A lane 8) indicated the formation of Y-DNA. Similar results were obtained from the one-pot synthesis of X-DNA and T-DNA.

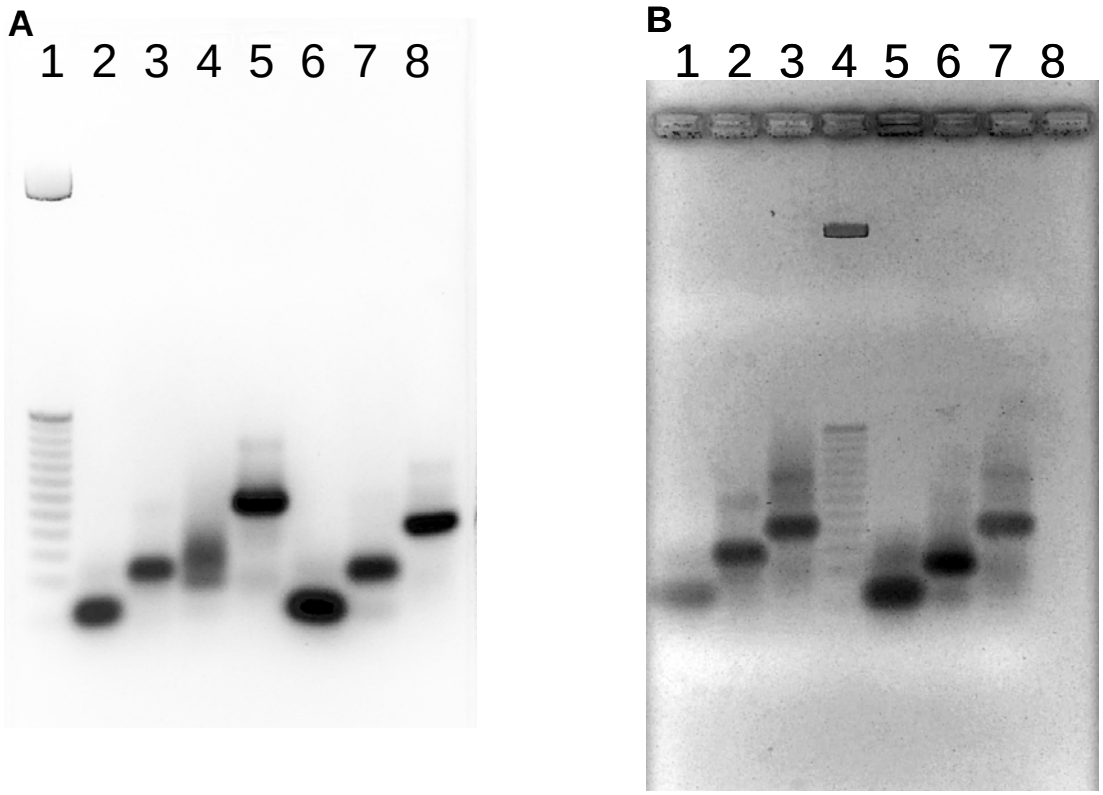

Figure 3.1. BDM Syntheses. **(A)** Evaluation of X_0-DNA and Y_0-DNA by 3% agarose gel. Lanes 1 is 25 bp DNA ladder. Lane 2 is oligonucleotide X_{0a}.Lanes 3 is the hybridized products of X_{0a} and $X_{0b.}$ Lane 4 is the hybridized products of $X_{0a,}$ X_{0b} and X_{0c}. Lanes 5 is hybridized final products of (X_{0a}, X_{0b}, X_{0c} and X_{0d}). Lane 6 is oligonucleotide Y_{0a} Lane 7 is hybridized products of (Y_{0a} and Y_{0b}) Lane 8 is hybridized final products of (Y_{0a}, Y_{0b} and Y_{0c}). **(B)** Evaluation of T_0-DNA by 3% agarose gel. Lane 1 is oligonucleotide $T_{0a.}$ Lane 2 is hybridized products of T_{0a} and $T_{0b.}$ Lane 3 is hybridized final products of T_{0a}, $T_{0b,}$ and $T_{0c.}$ Lane 4 is 25 bp DNA ladder. Lane 5 is oligonucleotide X_{0a}. Lanes 6 is the hybridized products of X_{0a} and $X_{0b.}$ Lanes 7 is hybridized final products of (X_{0a}, X_{0b} and X_{0c}).

BDM synthesized were used to synthesize DNA hydrogels, following the methods described above.

It has been shown that X-Gel swells the most, while Y-Gel and T-Gel swell similarly but less than X-Gel. These can be seen from the DNA hydrogel images shown in Figure 3.2. While all the DNA hydrogels are cylindrical and have the same diameter, X-Gel has the largest height, approximately 6 mm, compared to about 3 mm for Y-Gel and T-Gel. The difference in swelling is possibly due to the different molecular structure of these gels.

The dimensions of DNA hydrogels, as well as their volumes and surface areas, are summarized in Table 3.1. As X-Gel swells the most and thus has the largest height, it also has the largest volume and surface area, compared with Y-Gel and T-Gel.

The loading efficiency was deduced from the amounts of effectively incorporated and initially introduced proteins. As can be seen from Figure 3.3 and Figure 3.4, no significant difference among different DNA hydrogels was observed for the loading efficiencies of insulin and BSA, respectively. Compared to the loading efficiencies of insulin into DNA hydrogels, the loading efficiencies of BSA into DNA hydrogels are significantly lower compared with insulin. This is possibly due to the higher molecular weight and larger size of BSA. Also as insulin has a solubility of about 1 mg/ml in water at room temperature, BSA has a much higher solubility of 40 mg/ml. Thus BSA tends to stay more in the PBS buffer than insulin.

Insulin release experiments were conducted in a study period of 32 days. Smooth release curves were obtained, as can be seen from Figure 3.5. In particular, the release of insulin was dependent on the types of BDM. After 7 days, about 40%, 35% and 30% of insulin were release from Y-, T- and X-DNA gels, respectively. The total amount of insulin released within 32 days was 55%, 50% and 45% for Y-, T- and X-DNA gels, respectively.

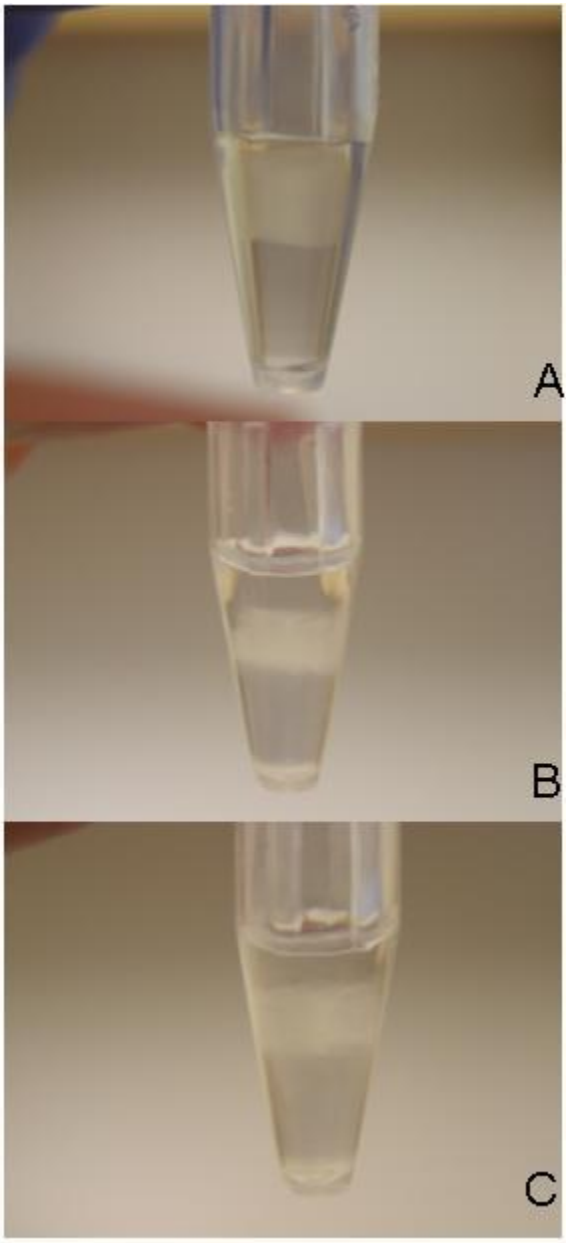

Figure 3.2. DNA hydrogels. (**A**) X-Gel (**B**) Y-Gel (**C)** T-Gel

Table 3.1. Dimensions of DNA hydrogels

	Height (mm)	Diameter (mm)	Volume (mm^3)	Surface Area (cm^2)
X-Gel	6.0	6.0	166	1.53
Y-Gel	3.0	6.0	83	1.12
T-Gel	3.0	6.0	83	1.12

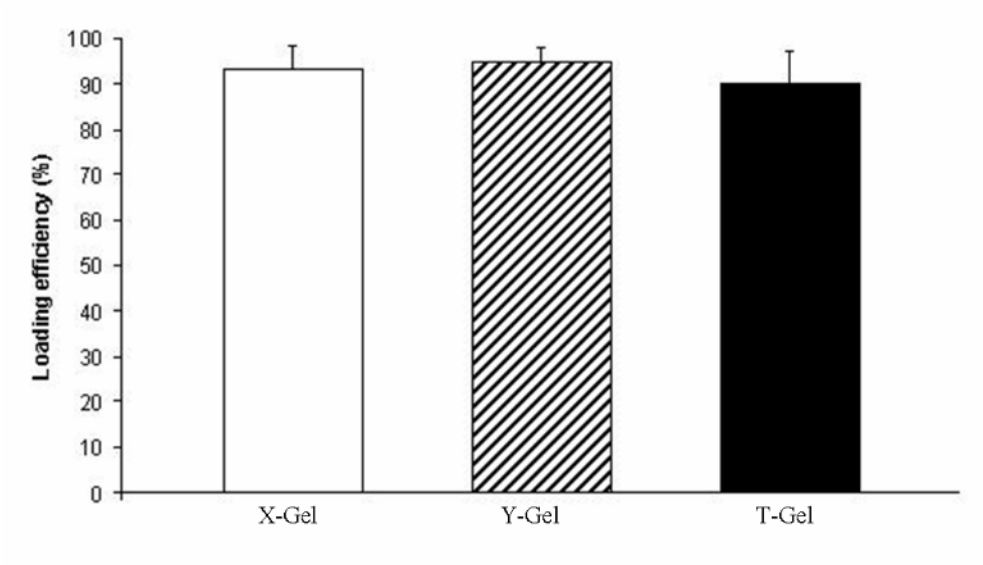

Figure 3.3. Loading efficiencies of insulin into different DNA hydrogels. The left, middle, and right bars are representing X-Gel, Y-Gel, and T-Gel, respectively. The error bars represent standard deviation from three or more replicates.

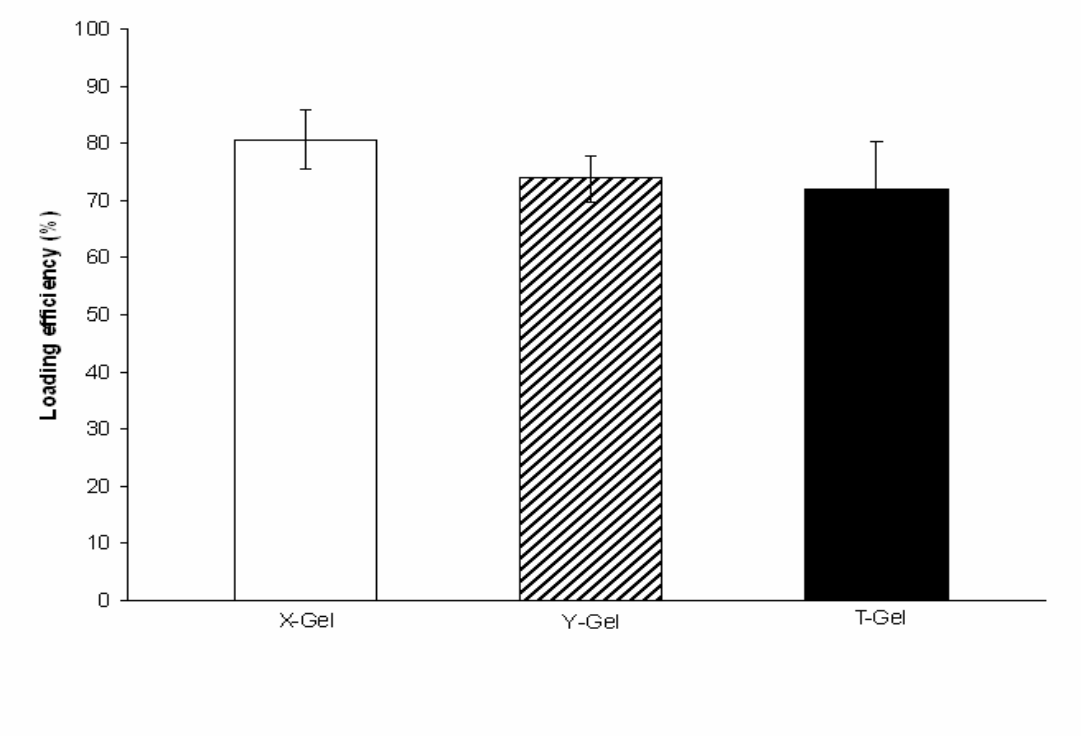

Figure 3.4. Loading efficiency of BSA into different DNA hydrogels. The left, middle, and right bars are representing X-Gel, Y-Gel, and T-Gel, respectively. The error bars represent standard deviation from three or more replicates.

BSA release experiments were conducted in a study period of 22 days. Although there was burst effect detected especially of Y- and T-DNA gels, smooth release curves were obtained, as can be seen from Figure 3.6. In particular, the release of BSA was dependent on the types of BDM. After 7 days, about 60%, 60% and 50% of BSA were release from Y-, T- and X-DNA gels, respectively. The total amount of BSA released within 22 days was 75%, 75% and 60% for Y-, T- and X-DNA gels, respectively.
The release difference may be attributed to and thus can be controlled by the structural variations in the DNA gels.

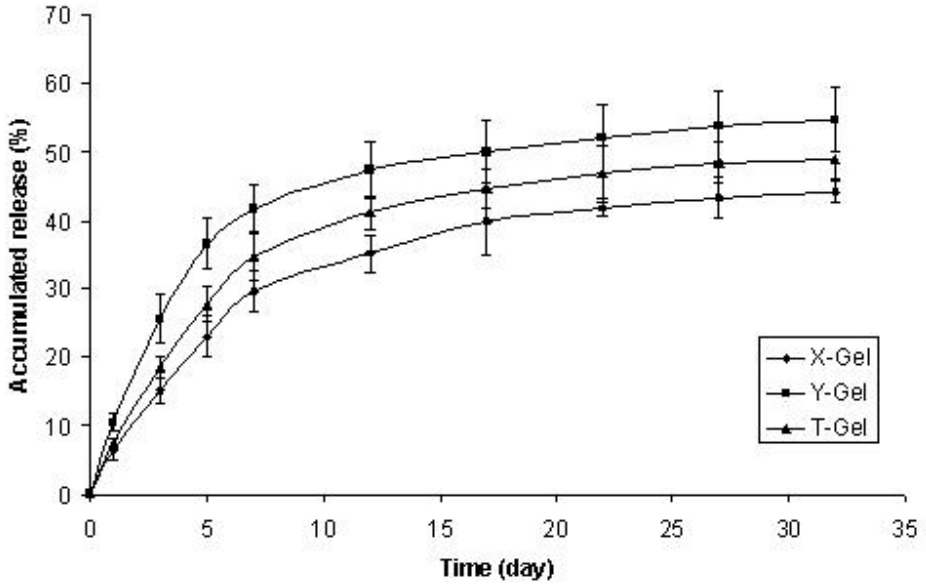

Figure 3.5. Controlled insulin release profiles of different DNA hydrogels. The diamonds, squares and triangles indicate X-, Y- and T-DNA gels. The error bars represent standard deviation from three or more replicates.

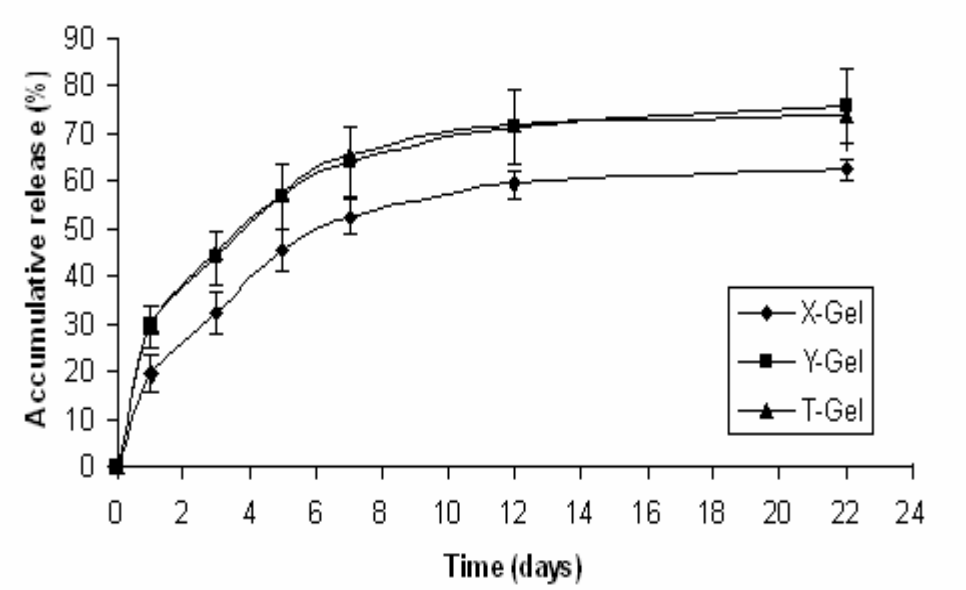

Figure 3.6. Controlled BSA release profiles of different DNA hydrogels. The diamonds, squares and triangles indicate X-, Y- and T-DNA gels. The error bars represent standard deviation from three or more replicates.

In order to investigate the mechanism of release, accumulated release amount is plotted against the square root of time. Figure 3.7 and Figure 3.8 show there is almost a linear relationship between accumulated release percentage of insulin and BSA, and the $t^{1/2}$ for the first week, respectively. This indicates the release is almost diffusion-controlled. The decrease in release rate in the following two weeks may due to the insufficient pathways for the release of insulin and BSA encapsulated deeply inside the hydrogels.

Incomplete release occurs when some of the drug particles are isolated, or completely surrounded by polymer. These drug molecules have no pathway to the surface. Large amount of insulin and BSA were still trapped inside the DNA hydrogels at the end of study period. Figure 3.9 shows after 32 days, about 30%, 20% and 20% of BSA were left in X-, Y-, and T- DNA gels, respectively. The leftover of insulin in X-, Y-, and T-DNA gels, respectively, are about 45%, 25% and 40%.This is possibly because the pore size formed upon swelling of the DNA hydrogels alone was not large enough for these large size proteins. The pore size of DNA hydrogels is at the nanometer scale and is supposed to around 13.2 nm theoretically. The hydrodynamic radius of insulin and BSA are 1.6 nm and 3.7 nm, respectively. Furthermore, it has been shown that insulin aggregates in aqueous solutions upon shaking. The pore size of DNA hydrogels may not be large enough for these insulin aggregates to pass through.

A schematic drawing of a cylindrical X-Gel used in the computer simulation is shown in Figure 3.10. The dimensions of Y-Gel and T-Gel used in the simulation would be the same as X-Gel, except that the height of Y-Gel and T-Gel is 3 mm, instead of 6 mm for X-Gel. As noted above, the crucial step in the simulation process is to calculate the amount of protein drugs inside DNA hydrogels at certain time points. This is done by calculating the concentration of the drugs, assuming there is a constant volume for DNA hydrogels.

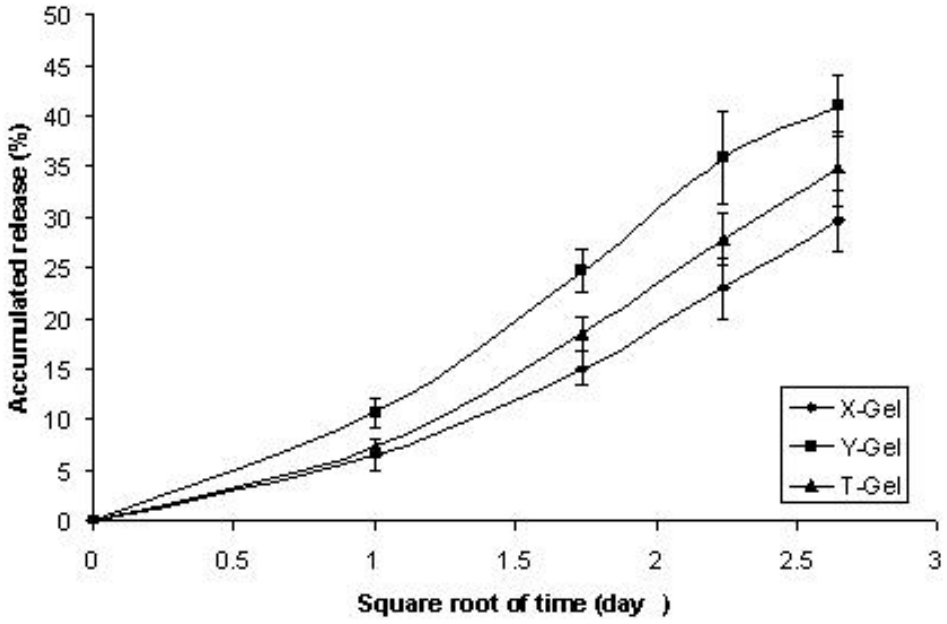

Figure 3.7. Cumulative release (%) of insulin from DNA hydrogels is proportional to the square root of time up to about 45% protein release. The diamonds, squares and triangles indicate X-, Y- and T-DNA gels. The error bars represent standard deviation from three or more replicates.

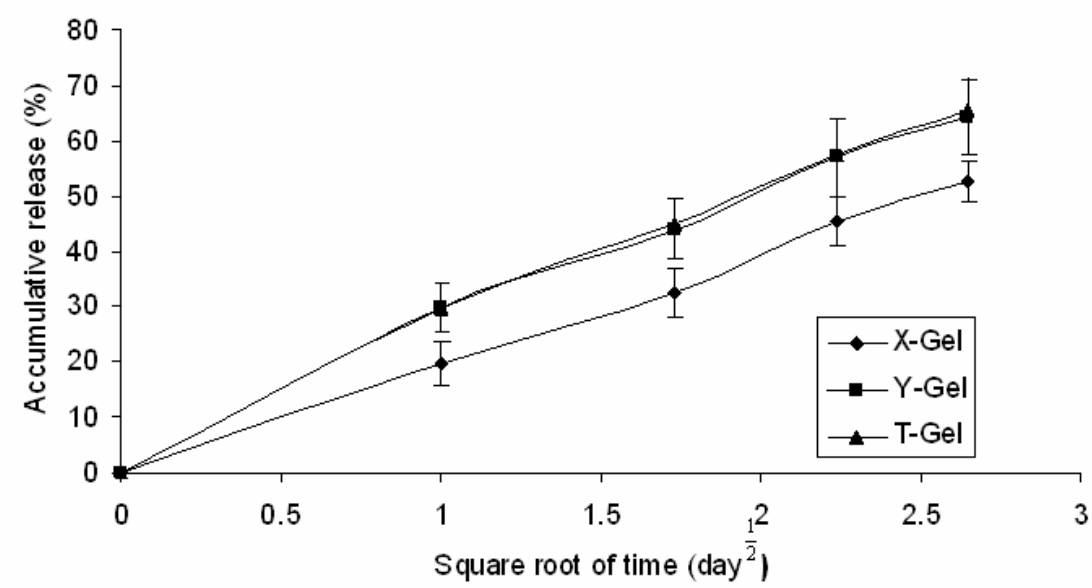

Figure 3.8. Cumulative release (%) of BSA from DNA hydrogels is proportional to the square root of time up to about 60% protein release. The diamonds, triangles and squares indicate X-, Y- and T-DNA gels. The error bars represent standard deviation from three or more replicates.

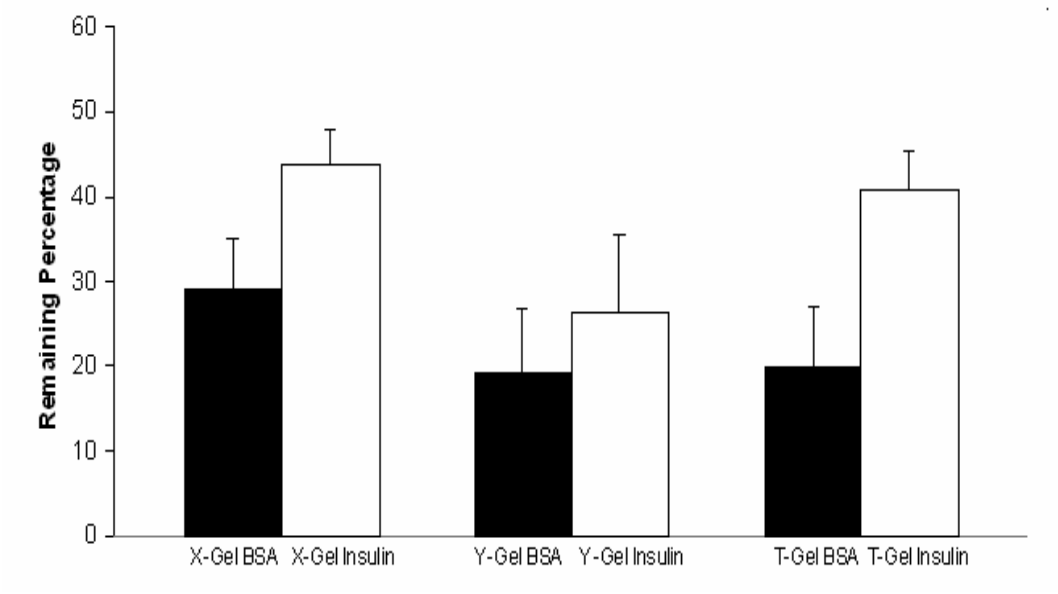

Figure 3.9. Amount of insulin and BSA left in DNA hydrogels after 32 days. Black bars represent the amount of BSA remaining in DNA hydrogels while white bars represent the amount of insulin remaining in DNA hydrogels.

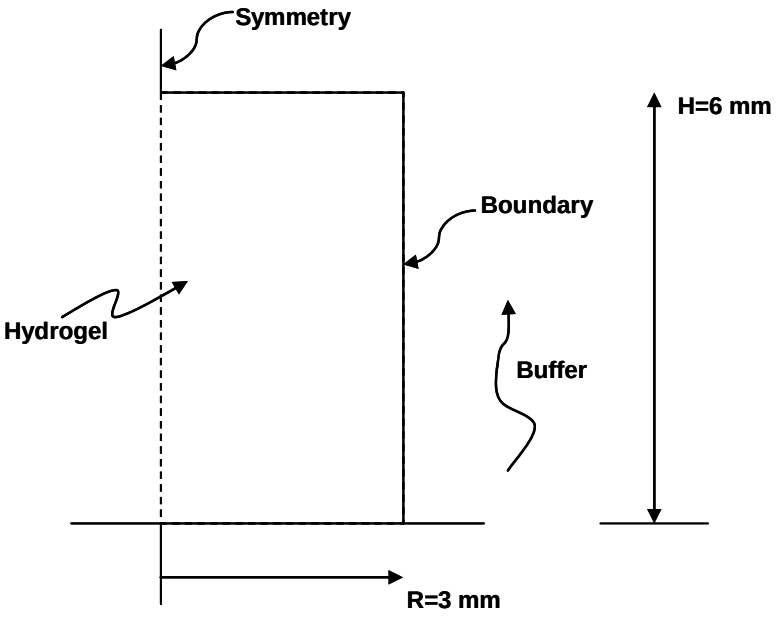

Figure 3.10. A schematic of a cylindrical X-Gel used in the simulation, showing dimensions and boundary conditions.

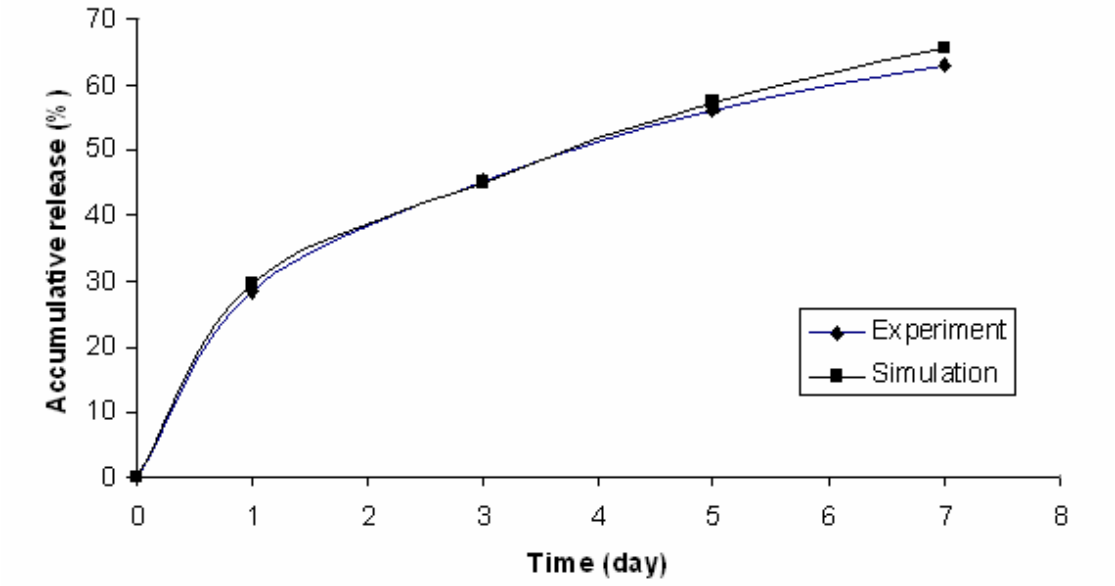

Figure 3.11. Computer simulation of BSA release from T-Gel. The diamonds and squares indicate experimental release data of T-DNA gel and computer simulation for T-DNA gel, respectively.

Figure 3.11 shows the results of FEM solution to equation (2.1). Figure 3.11 shows the simulation agrees well with the experimental data of BSA release from T-DNA gel for the first week. Other simulation results also showed good agreement with the release experiment data for the first week for both insulin and BSA (data not shown). This confirms the mechanism for the release in the first week is diffusion controlled. However the diffusion model can not be applied to the entire study period of 32 days for insulin and 22 days for BSA, Figure 3.12 shows apparent discrepancy remains between the simulation and the experimental data of insulin release from Y-Gel after the first week. Other simulation results also showed discrepancy between the simulation and the experimental data (data not shown).

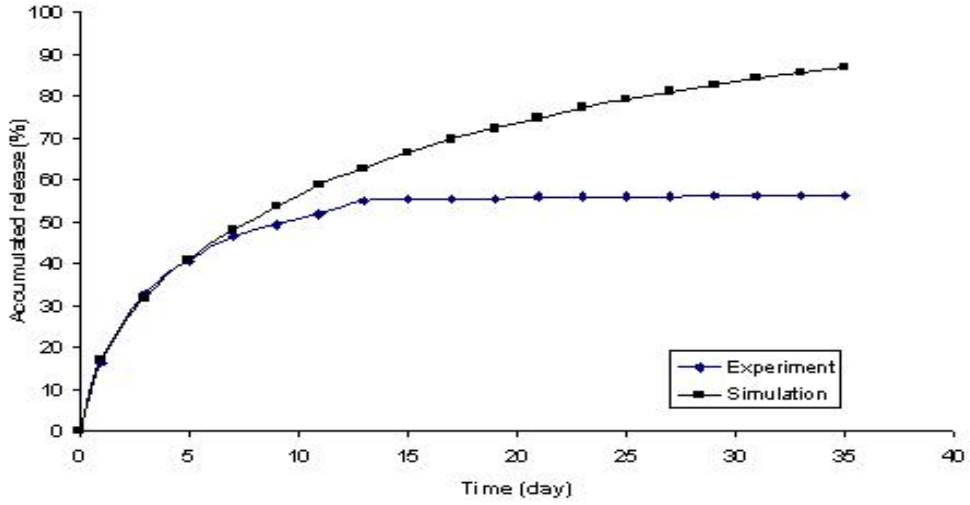

Figure 3.12. Computer simulation of insulin release from Y-Gel. The diamonds and squares indicate experimental release data of Y-DNA gel and computer simulation for Y-DNA gel, respectively.[1]

[1] The optimization work starting on this page and continuing for the following four pages, including Figure 3.13, is the work of Dr. E. Balsa-Canto and Dr. J. Banga of the Process Eng. Group, I.I.M.-C.S.I.C, C/Eduardo Cabello 6, 36208, Vigo, Spain..

Since a constant diffusivity of proteins in the gel could not explain the release profiles, a varying diffusivity with concentration was tried. An optimization procedure was used to arrive at a diffusivity variation with concentration that best describes the measured data. For the optimization, numerical method of lines was used. Second order formulas with a discretization level of 11x11 were used as a first guess. The resulting set of ordinary differential equations (ODEs) is solved using a stiff ODE solver RADAU5[5]. The coarse grid of 11x11 was needed to reduce computational time since a large number of model evaluations were required. Refined solutions were calculated on a finer grid (15x15). For optimization, a global method[6] is used.

A quadratic variation of diffusivity with concentration, *c*, provided good fit of the predictions with experimental data but, when extrapolated beyond the range used in the optimization process, predicted negative diffusivities for low concentrations. Therefore, an exponential variation in diffusivity with concentration, of the form $D = a_1(1 - \mathrm{e}^{a_2 c})$ was used instead. For the three gels, diffusivity variation given in Eqn.(3.1) provided the least sum of squares computed between measured release and the release predicted by the model:

$$D = \begin{cases} -0.000301201(1 - e^{0.0785728c}) \text{ for X-gel} \\ -0.00120246(1 - e^{0.0722563c}) \text{ for Y-gel} \\ -0.00062646(1 - e^{0.073535c}) \text{ for T-gel} \end{cases} \tag{3.1}$$

Comparison between measured and the predicted release for the above diffusivities are shown in Figure 3.13.

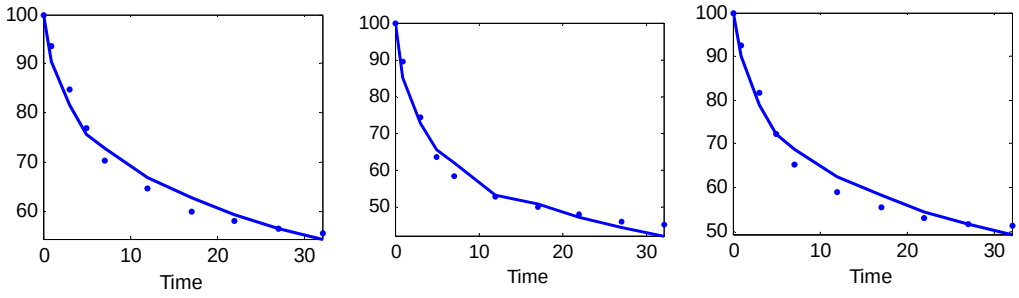

Figure 3.13. Measured release (points) and predicted release (solid lines) for the diffusivity variations with concentration shown in Eqn.(3.1), for X-gel, Y-gel and T-gel, respectively.

To improve understanding of these diffusivity variations with concentration in terms of their magnitudes and relative variations in different gels, relationships in Eqn.(3.1) are plotted in Figure 3.14. From this figure for diffusion of insulin, X-Gel has the smallest diffusivity while compared to Y-Gel and T-Gel. It has been shown that among the three types of DNA hydrogels, X-Gel has the largest tensile modulus and is most resistant to degradation[3]. This is possibly due to the unique molecular structure of X-Gel as each X-DNA building block has four arms which could be cross-linked to other X-DNA building blocks, compared to the three arms of Y-DNA and T-DNA building blocks. This not only makes X-Gel much stronger, but more difficult for the proteins drugs to diffuse through.

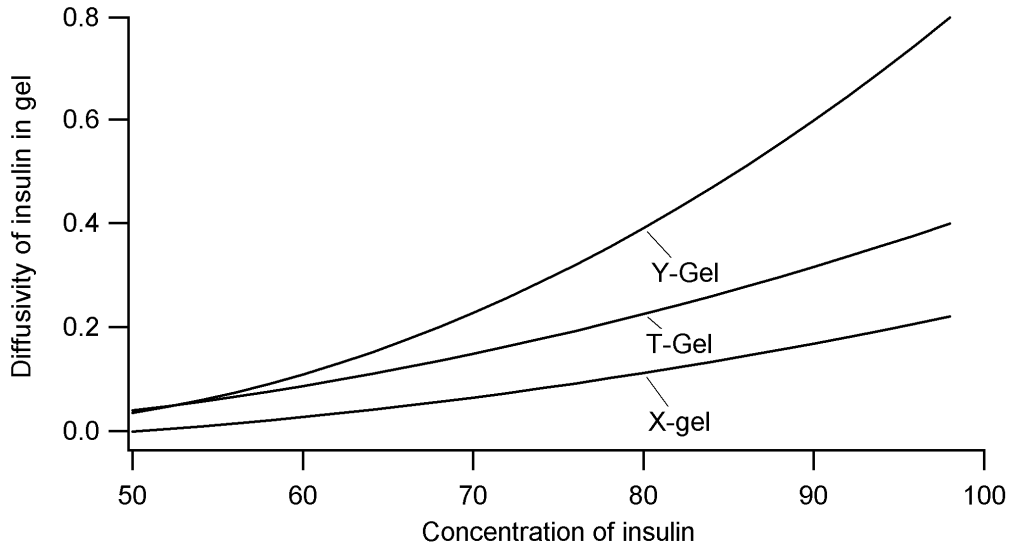

Figure 3.14. Concentration-dependent diffusivities of insulin in DNA hyrogels

3.2 Discussions

A useful method of comparing the protein release from different hydrogel materials is to calculate the effective diffusion coefficient, D_e. We found that there are significant decreases in D_e of insulin and BSA in these DNA hydrogels compared to the infinite-dilution diffusion coefficients, D_0. For insulin, our simulation showed its diffusivities in DNA hydrogels are approximately $1\times10^{-11}\,m^2/s$, which is smaller than the reported infinite dilution diffusivity $7.7\times10^{-11}\,m^2/s$[7].

Our experimental findings showed that the D_e of BSA was generally larger than that of insulin. One possible reason for this may be attributed to the higher solubility of BSA in water (40 mg/mL) than that of insulin (1 mg/mL). Another possible reason is increasing protein size increases the rate of protein release. The size of the proteins in the matrix affects the size of the water-filled channels formed as the particle dissolve. Larger particles occupy more volume in a matrix, increasing the pore-to-pore connectivity. Increased connectivity provides simpler pathways (i.e., less tortuous and less constricted pathways) for diffusion of protein drugs. As the hydrodynamic radius of BSA monomer is about 3.7 nm, while insulin monomer has a hydrodynamic radius of about 1.3 nm, it is possible that this size difference would have an effect on the diffusivity difference between BSA and insulin in DNA hydrogels.

REFERENCES

1. R. T. Bartus, M. A. Tracy, D. F. Emerich, and S. E. Zale. Drug Delivery: sustained delivery of proteins for novel therapeutic products, *Science*, **281**, 1161-1162 (1998)
2. N. Kumar, R. S. Langer and A. J. Domb. Polyanhydrides: an overview, *Advanced Drug Delivery Reviews*, **54,** 889-910, (2002)
3. S. H. Um, J. B. Lee, N. Park, S. Y. Kwon, C. C. Umbach and D. Luo. Enzyme-catalysed assembly of DNA hydrogel, *Nature Materials*, **5**, 797-801 (2006)
4. Y. Li, Y.D. Tseng, S.Y. Kown, L. d'Espaux, J.S. Bunch, P.L McEuen and D. Luo. Controlled assembly of dendrimer-like DNA, *Nature Materials*, **3**, 38-42 (2004)
5. A. Hairer and G. Wanner. Solving ordinary differential equations. Stiff and Differentialalgebraic Problems. 2nd Edition. Springer Series in Computation Mathematics, **14**, (1996)
6. J. A. Egea, M. Rodriguez-Fernandez, J. R. Banga and R. Marti. Scatter Search for Chemical and Bio-Process Optimization, *Journal of Global Optimization*, **37** (3), 481-503, (2007)
7. M. V. Sefton and E. Nishimura. Insulin permeability of hydrophilic polyacrylate membranes, *Journal of Pharmaceutical Sciences*, **69** (2), 208-209, (1980)

Chapter 4
Conclusions and Future work

4.1 Conclusions

In conclusion, three types of DNA hydrogels have been synthesized. Release characteristics of two protein drugs, insulin and BSA, have been studied. Over one month period, smooth release curves have been observed. The release kinetics is dependent on the type of DNA hydrogel. X-Gel has the slowest release rate for both insulin and BSA.

The release mechanism of insulin and BSA from DNA hydrogels were appropriately and simply described by the diffusion model in the first week. The diffusion model would not be able to describe the release profiles after the first week. This is possibly due to the degradation of DNA hydrogels and aggregation of proteins inside DNA hydrogels. An exponential fit using a concentration-dependent diffusivity provided good agreement between the simulation and the experimental data.

DNA hydrogels can be easily tuned to have different molecular structures at the nanometer scale and various sizes in the macroscale range. They can be ideal candidates for biodegradable, biocompatible and controlled drug delivery systems. Considering the availability of a vast number of enzymes that can manipulate DNA at angstrom scale, our results strongly suggest that DNA can be engineered as a designer material whose properties can be more easily tuned. These biodegradable, biocompatible, DNA hydrogels are a new class of materials that can be exploited in a variety of biomedical applications including sustained drug delivery, tissue engineering, 3D cell culture, cell transplant therapy and other biomedical applications[1].

Future work includes using dynamic light scattering to study insulin aggregation under the same experimental conditions. Different sizes and shapes of DNA hydrogels can also be tuned to optimize the release characteristics of these protein drugs.

REFERENCES

1. S. H. Um, J. B. Lee, N. Park, S. Y. Kwon, C. C. Umbach and D. Luo. Enzyme-catalysed assembly of DNA hydrogel, *Nature Materials*, **5**, 797-801 (2006)

APPENDIX A

Encapsulation Efficiency of Protein Drugs in DNA Hydrogels

Insulin

	Average Encapsulation Efficiency	Standard Deviation
X-Gel	93.12	5.125781
Y-Gel	95.08	3.085023
T-Gel	90.03	7.140198

BSA

	Average Encapsulation Efficiency	Standard Deviation
X-Gel	80.66	5.20781
Y-Gel	73.83	4.20311
T-Gel	72.09	8.16798

APPENDIX B

Accumulated Release Percentage of Protein Drugs from DNA Hydrogels

Insulin

Day	Square Root of Time	X-Gel Accumulated %	X-Gel Standard Deviation	Y-Gel Accumulated %	Y-Gel Standard Deviation	T-Gel Accumulated %	T-Gel Standard Deviation
0	0	0	0	0	0	0	0
1	1	6.483333	1.52902	10.490000	1.39689	7.41666667	0.61158
3	1.73205	15.086667	1.78215	25.560000	3.5921	18.4833333	1.67837
5	2.23607	22.976667	2.96380	36.5366667	3.69635	27.770000	2.48387
7	2.64575	29.696667	3.00976	41.6666667	3.57878	34.810000	3.60529
12	3.4641	35.173330	2.67489	47.2866667	4.12835	41.0866667	2.39061
17	4.12311	39.830000	4.80392	50.0166667	4.58839	44.6366667	2.83507
22	4.69042	41.916667	1.09501	51.9866667	5.03613	46.8933333	4.10968
27	5.19615	43.426667	2.99367	53.7833333	5.04256	48.4133333	2.94376
32	5.65685	44.223330	1.57233	54.680000	4.79832	48.8533333	2.68683

BSA

Day	Square Root of Time	X-Gel Accumulated %	X-Gel Standard Deviation	Y-Gel Accumulated %	Y-Gel Standard Deviation	T-Gel Accumulated %	T-Gel Standard Deviation
0	0	0	0	0	0	0	0
1	1	19.68	3.8925442	29.6433333	4.4189856	29.6433333	4.418986
3	1.732	32.60333333	4.37788	43.9933333	5.470003	45.2	3.002466
5	2.236	45.57666667	4.4128336	56.9133333	6.8867288	57.4866667	5.952515
7	2.646	52.68666667	3.713655	64.3266667	6.9859597	65.6233333	5.986989
12	3.464	59.52	2.7923168	71.5866667	7.6453406	72.0366667	3.743158
22	4.69	62.60333333	2.2601401	75.9733333	7.6357864	73.86	4.544128

APPENDIX C

Remaining Percentage of Protein Drugs in DNA Hydrogels

Insulin

	Remaining Percentage	Standard Deviation
X-Gel	43.85	4.16
Y-Gel	26.36	9.29
T-Gel	40.82	4.78

BSA

	Remaining Percentage	Standard Deviation
X-Gel	29.04	5.94
Y-Gel	19.02	7.81
T-Gel	19.95	7.20